

# *A Frequency-Sweep Based Load Monitoring Method for Weakly-Coupled Series-Series Compensated Wireless Power Transfer Systems*

Yun Yang

Department of Electrical and  
Electronic Engineering  
The University of Hong Kong  
Hong Kong, China  
yangyun@eee.hku.hk

Yajie Jiang

Department of Electrical and  
Electronic Engineering  
Huazhong University of Science  
and Technology  
Wuhan, China  
yajiejjiang@hust.edu.cn

Siew-Chong Tan

Department of Electrical and  
Electronic Engineering  
The University of Hong Kong  
Hong Kong, China  
sctan@eee.hku.hk

Shu-Yuen Ron Hui

Department of Electrical and  
Electronic Engineering  
The University of Hong Kong  
Hong Kong, China  
ronhui@eee.hku.hk

**Abstract**—In this paper, a frequency-sweep based load monitoring method is proposed for weakly-coupled series-series (SS) compensated wireless power transfer (WPT) systems. By only measuring the input voltage and current of the transmitter coil, the proposed monitoring method can estimate the load resistance without any feedback signals from the receiver even for mid-range applications with very small coupling coefficients. Compared to the existing monitoring methods for short-range applications, the proposed monitoring method uses a simpler estimation equation. Both simulation and experimental results are included to confirm that the proposed monitoring method can accurately estimate load resistances of weakly-coupled SS compensated WPT systems.

**Keywords**—load monitoring, series-series (SS) compensated wireless power transfer (WPT) system, estimation equation.

## I. INTRODUCTION

The pioneering wireless power transfer research of Nikola Tesla based on the use of high frequency and magnetic resonance in 1893 [1] has received renewed interests over the last two decades. Near-field wireless power transfer (WPT) based on the magnetic resonant coupling has been widely investigated for applications in medical implants [2]–[5], induction heaters [6], electric vehicles [7]–[10], and portable devices [11]–[13]. Since 2010, WPT techniques have been commercialized for the portable devices based on the “Qi” standard [14], which is now used by over 500 companies in the Wireless Power Consortium.

WPT systems can operate under either the maximum power transfer (MPT) principle or the maximum energy efficiency (MEE) principle [15]. It has been pointed out that the MPT principle should be adopted for mid-range applications only for very low-power ( $\mu$ W) applications, such as wireless powered sensors. For wireless power applications higher than a few Watts, such as portable consumer electronics and electric vehicles, the MEE principle should be adopted for high-efficiency transmissions. Regardless of which WPT principle

to be adopted, control schemes without the requirement of wireless feedbacks from the receiver circuit are preferable because it can reduce costs and simplify circuitry [16]–[21]. For high-performance dynamic control designs, the load conditions have to be monitored in real time [17].

By far, several load monitoring methods are used for WPT systems [18]–[21]. In [18], an energy equilibrium function of a zero-voltage switching (ZVS) for a two-coil system is introduced to estimate load variations. In [19], a simplified model of a parallel-parallel (PP) compensated WPT system at the fixed resonant frequency is adopted to derive the load power by measuring only the input voltage and current. In [20], a transient model of a series-series (SS) compensated WPT system is used to detect the initial load condition by injecting a series of high-frequency signals before startup. In [21], the load resistance can be determined by measuring the input voltage and current at one frequency only. However, these methods are primarily designed for strongly-coupled WPT systems for short-range applications.

Front-end or primary-side monitoring method for mid-range applications in which the magnetic coupling coefficient is very small has not been fully explored. In this paper, a frequency-sweep based load monitoring method is proposed to monitor load conditions of weakly-coupled series-series (SS) compensated WPT systems at both short-range and mid-range by only measuring the input voltage and the transmitter current. An analysis is presented to highlight the conditions under which the proposed method can be applied accurately. Compared to the existing front-end monitoring strategies, the proposed load monitoring method has two advantages. First, the estimation equation is very simple, making it suitable for implementation in low-cost digital controllers for feedback control designs. Second, its accuracy in practical applications can be improved by reducing the estimation errors of some parameters via frequency sweep in a wide spectrum.

This work was supported by Hong Kong Research Grant Council under theme-based Research Project T23-701/14-N.

## II. DERIVATIONS OF THE LOAD ESTIMATION EQUATION

The equivalent circuit of a typical SS compensated WPT system is shown in Fig. 1. Here,  $L_p$  and  $L_s$  are the self-inductances of the primary and the secondary coils;  $R_p$  and  $R_s$  are their parasitic resistances;  $C_p$  and  $C_s$  are the compensation capacitors, respectively;  $R_L$  is the load resistance or the equivalent load resistance;  $v_{in}$  is the input voltage;  $i_p$  and  $i_s$  are the currents of the transmitter and the receiver;  $v_{cp}$  and  $v_{cs}$  are the voltages of the compensated capacitors, respectively.

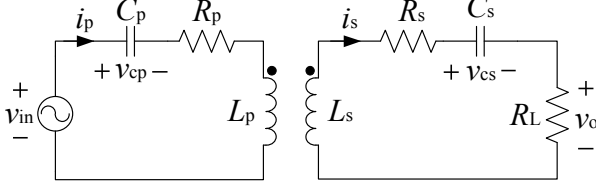


Fig. 1. Equivalent circuit of a typical SS compensated WPT system.

Based on the Kirchhoff's law,

$$\begin{cases} v_{in} = v_{cp} + R_p i_p + L_p \frac{di_p}{dt} - M \frac{di_s}{dt} \\ i_p = C_p \frac{dv_{cp}}{dt} \\ 0 = v_{cs} + (R_s + R_L) i_s + L_s \frac{di_s}{dt} - M \frac{di_p}{dt} \\ i_s = C_s \frac{dv_{cs}}{dt} \end{cases}, \quad (1)$$

where  $M$  is the mutual inductance between the primary and the secondary coils;  $\omega$  is the angular frequency of the input voltage. By applying the extended describing function (EDF) method [22],

$$\begin{cases} v_{in} = V_{in} \sin(\omega t) \\ i_p = I_{ps} \sin(\omega t) + I_{pc} \cos(\omega t) \\ v_{cp} = V_{cps} \sin(\omega t) + V_{cpc} \cos(\omega t) \\ i_s = I_{ss} \sin(\omega t) + I_{sc} \cos(\omega t) \\ v_{cs} = V_{css} \sin(\omega t) + V_{csc} \cos(\omega t) \end{cases} \quad (2)$$

The compensation capacitor  $C_p$  of the transmitter coil-resonator is designed to nullify the primary inductance  $L_p$  for minimizing the apparent power rating of the power supply [23] and the compensation capacitor  $C_s$  of the receiver coil-resonator is designed to nullify the secondary inductance  $L_s$  for maximizing the transfer capability [24].

$$\begin{cases} C_s = \frac{1}{\omega_o^2 L_s} \\ C_p = \frac{1}{\omega_o^2 L_p} \end{cases}, \quad (3)$$

where  $\omega_o$  is nominal angular frequency of the input voltage.

Substituting (2) and (3) into (1) and simplifying the equation by cancelling the terms  $I_{ss}$  and  $I_{sc}$ , the system equation can be obtained as follows:

$$\begin{bmatrix} R_p I_{pc} + Z_p I_{ps} & a^2 \omega_o^2 I_{pc} \\ R_p I_{ps} - Z_p I_{pc} - V_{in} & a^2 \omega_o^2 I_{ps} \end{bmatrix} \begin{bmatrix} R_s + R_L \\ M^2 \end{bmatrix} = \begin{bmatrix} Z_s V_{in} + Z_p Z_s I_{pc} - R_p Z_s I_{ps} \\ Z_p Z_s I_{ps} + R_p Z_s I_{pc} \end{bmatrix}, \quad (4)$$

where  $a$  is the frequency ratio,  $Z_p = \left(\frac{a^2-1}{a}\right) \omega_o L_p$ , and  $Z_s = \left(\frac{a^2-1}{a}\right) \omega_o L_s$ .

Based on (4),

$$R_L = \frac{Z_s V_{in} I_{ps} - R_p Z_s (I_{ps}^2 + I_{pc}^2)}{V_{in} I_{pc} + Z_p (I_{ps}^2 + I_{pc}^2)} - R_s. \quad (5)$$

For  $i_p = I_p \sin(\omega t + \theta)$ , where  $\theta$  is the phase angle between the input voltage and the transmitter current, it can be decomposed into two components,

$$\begin{cases} I_{ps} = I_p \cos \theta \\ I_{pc} = I_p \sin \theta \end{cases}. \quad (6)$$

Substituting (6) into (5),

$$R_L = \frac{Z_s V_{in} \cos \theta - R_p Z_s I_p}{V_{in} \sin \theta + Z_p I_p} - R_s \quad (a \neq 1). \quad (7)$$

Ideally, the load resistance  $R_L$  can be estimated based on (7) by only measuring the input voltage ( $V_{in}$ ) and the transmitter current ( $I_p$ ) of the WPT system at one side frequency ( $a \neq 1$ ). However, the parasitic resistances  $R_p$  and  $R_s$  and the self-inductances  $L_p$  and  $L_s$  may vary at different operating frequencies. Using the measured parameters at the resonant frequency ( $a=1$ ) may result in considerable load estimation errors. To reduce the estimation errors, the estimated load resistances are averaged in a wide frequency spectrum as

$$\tilde{R}_L = \frac{1}{N} \sum_{i=1}^N \frac{Z_{si} V_{in} \cos \theta_i - R_{pi} Z_{si} I_{pi}}{V_{in} \sin \theta_i + Z_{pi} I_{pi}} - R_{si} \quad (a \neq 1). \quad (8)$$

## III. SIMULATION RESULTS

Simulations are carried out in MATLAB/SIMULINK with the specifications of the SS compensated WPT system given in Table I. The resonant frequency of the WPT system is set at 100 kHz. The mutual inductances are measured in the experimental setup with the distances between the transmitter and receiver coils varying from 8 cm to 10 cm by the interval of 2 cm (listed in Table II). Six cases of input voltages and actual load resistances with variable mutual inductances in Table II are investigated, as shown in Table III. The schematic diagram in the SIMULINK is shown in Fig. 2. In the simulation study, the input power is considered to be supplied by a DC microgrid, which is generally 48 V or 400 V. Therefore, according to the EDF [22],  $V_{in}$  is set as 61.12 V or 509.3 V.

TABLE I. SPECIFICATIONS OF THE SS COMPENSATED WPT SYSTEM

Parameter	Value	Parameter	Value
$L_p$	91.926 $\mu\text{H}$	$C_p$	27.555 nF
$R_p$	0.474 $\Omega$	$L_s$	91.058 $\mu\text{H}$
$C_s$	27.818 nF	$R_s$	0.733 $\Omega$

TABLE II. MUTUAL INDUCTANCES FOR DIFFERENT DISTANCES BETWEEN THE COILS

No.	Distance (cm)	$M$ ( $\mu\text{H}$ )	No.	Distance (cm)	$M$ ( $\mu\text{H}$ )
1	8	19.382	10	26	3.68
2	10	15.515	11	28	3.15
3	12	12.333	12	30	2.721
4	14	10.194	13	32	2.384
5	16	8.431	14	34	2.08
6	18	7.021	15	36	1.828
7	20	5.935	16	38	1.621
8	22	5.017	17	40	1.459
9	24	4.306			

TABLE III. SIX CASES STUDIED IN SIMULATION

Case No.	$V_{in}$ (V)	$R_L$ ( $\Omega$ )	Case No.	$V_{in}$ (V)	$R_L$ ( $\Omega$ )
A	61.12	1	D	509.3	1
B	61.12	10	E	509.3	10
C	61.12	50	F	509.3	50

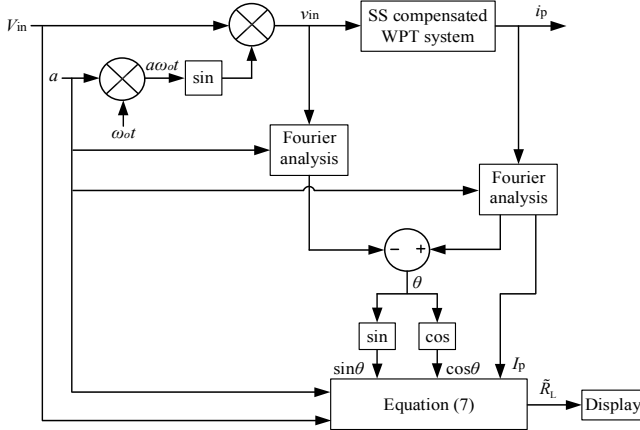
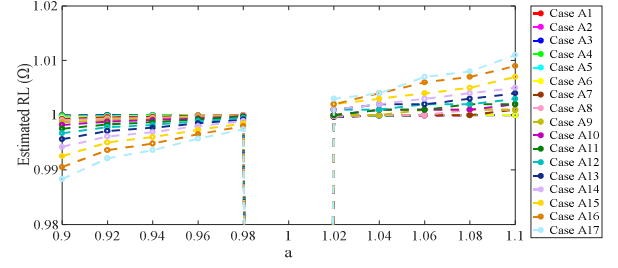


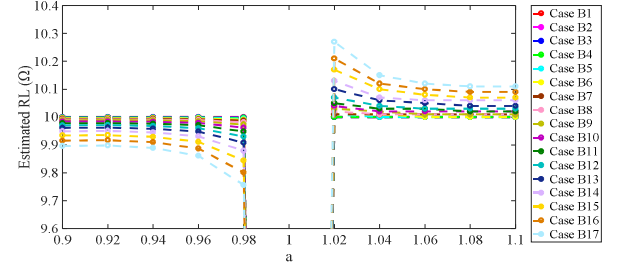
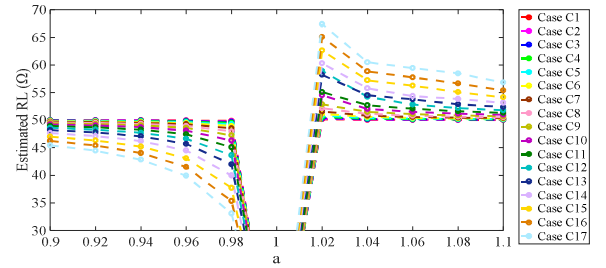
Fig. 2. Schematic diagram in SIMULINK.

For case A with  $V_{in}=61.12$  V,  $R_L=1$   $\Omega$ , and the mutual inductances listed in Table II, the switching frequency of the WPT system is swept from 90 kHz ( $a=0.9$ ) to 110 kHz ( $a=1.1$ ) with the interval of 2 kHz ( $\Delta a=0.02$ ), except the resonant

frequency ( $a=1$ ). The estimated  $R_L$  are shown in Fig. 3. Here, Case A1 indicates the estimated  $R_L$  for the distance of 8 cm and Case A17 indicates the estimated  $R_L$  for the distance of 40 cm. The averaged estimated  $R_L$  are provided in Table IV.

Fig. 3. Estimated  $R_L$  for the WPT system with  $V_{in}=61.12$  V and  $R_L=1$   $\Omega$ .

Simulations are also carried out for Case B, Case C, Case D, Case E, and Case F. The estimated  $R_L$  are shown in Figs. 4~8, respectively. The averaged estimated  $R_L$  are listed in Table IV. Apparently, the proposed method can accurately monitor load conditions of the SS compensated WPT system with various input voltages and load resistances. For  $R_L=1$   $\Omega$  and  $R_L=10$   $\Omega$ , the averaged estimation errors are 0.0026% and 0.0118%, respectively. For  $R_L=50$   $\Omega$ , the averaged estimation errors are 0.3992% and 0.3987% for case C and case F, respectively. Besides, for  $R_L=1$   $\Omega$ , the estimations at the frequency higher than the resonant frequency ( $a>1$ ) are slightly more accurate than the estimations at the frequency lower than the resonant frequency ( $a<1$ ). Conversely, for  $R_L=10$   $\Omega$  and  $R_L=50$   $\Omega$ , the estimations at the frequency lower than the resonant frequency ( $a<1$ ) are slightly more accurate than the estimations at the frequency higher than the resonant frequency ( $a>1$ ). Nevertheless, the estimation errors for  $a>1$  and  $a<1$  are consistently close and small.

Fig. 4. Estimated  $R_L$  for the WPT system with  $V_{in}=61.12$  V and  $R_L=10$   $\Omega$ .Fig. 5. Estimated  $R_L$  for the WPT system with  $V_{in}=61.12$  V and  $R_L=50$   $\Omega$ .

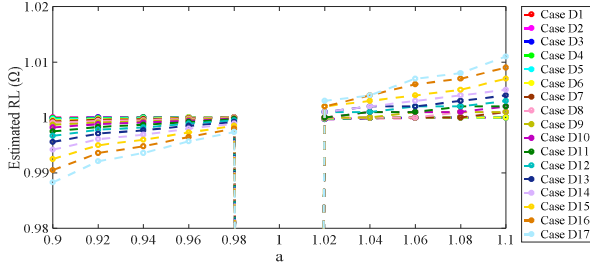


Fig. 6. Estimated  $R_L$  for the WPT system with  $V_m=509.3$  V and  $R_L=1$   $\Omega$ .

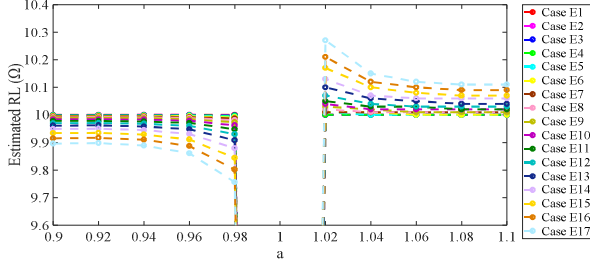


Fig. 7. Estimated  $R_L$  for the WPT system with  $V_m=509.3$  V and  $R_L=10$   $\Omega$ .

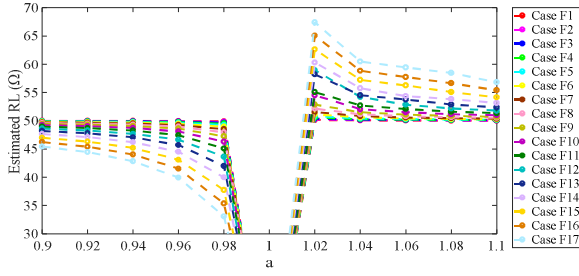


Fig. 8. Estimated  $R_L$  for the WPT system with  $V_m=509.3$  V and  $R_L=50$   $\Omega$ .

TABLE IV. AVERAGED ESTIMATED LOAD RESISTANCES IN SIMULATION

Case No.	Actual $R_L$ ( $\Omega$ )	Estimated $R_L$ for $a < 1$ ( $\Omega$ )	Estimated $R_L$ for $a > 1$ ( $\Omega$ )	Overall Estimated $R_L$ ( $\Omega$ )	Overall Relative Error (%)
A	1	0.998385882 (0.1614%)	1.001561176 (0.1561%)	0.999973529	0.0026
B	10	9.964470588 (0.3553%)	10.03788235 (0.3788%)	10.00117647	0.0118
C	50	47.49341176 (5.2778%)	52.90576471 (5.4923%)	50.19958824	0.3992
D	1	0.998385882 (0.1614%)	1.001561176 (0.1561%)	0.999973529	0.0026
E	10	9.964470588 (0.3553%)	10.03788235 (0.3788%)	10.00118235	0.0118
F	50	47.49305882 (5.0139%)	52.90564706 (5.8113%)	50.19935294	0.3987

#### IV. EXPERIMENTAL VERIFICATION

Experiments are carried out in an SS compensated WPT system with the specifications given in Table I and  $V_m=6.37$  V,  $R_L=10$   $\Omega$ , and the mutual inductances in Table II. The estimated  $R_L$  are shown in Fig. 9. It can be seen that the largest estimation error is less than 2%.

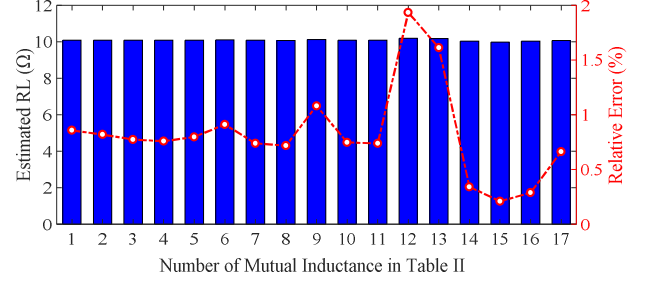


Fig. 9. Estimated  $R_L$  for the WPT system with  $V_m=6.37$  V and  $R_L=10$   $\Omega$  in experiment.

#### V. CONCLUSION

This paper proposes a frequency-sweep based front-end load monitoring method to estimate load resistances of weakly-coupled series-series (SS) compensated wireless power transfer (WPT) systems with very low mutual inductance (magnetic coupling coefficients). Retaining the advantages of existing front-end or primary-side monitoring methods, the proposed method can reduce estimation error by averaging the estimated parameters over a frequency range away from the resonant frequency. Both simulation and experimental results have confirmed that the load estimation errors are small by adopting the proposed method.

#### REFERENCES

- [1] N. Tesla, "On light and other high frequency phenomena," Philadelphia: Lecture Delivered before the Franklin Institute, Feb. 1893, and St. Louis, MO: before the National Electric Light Association, Mar. 1893. [online]. Available: [www.tfcbooks.com/tesla/](http://www.tfcbooks.com/tesla/).
- [2] B. Choi, J. Nho, H. Cha, T. Ahn and S. Choi, "Design and implementation of low-profile contactless battery charger using planar printed circuit board windings as energy transfer device," *IEEE Tran. Ind. Electron.*, vol. 51, no. 1, pp. 140–147, Feb. 2004.
- [3] W. H. Ko, S. P. Liang, and C. D. F. Fung, "Design of rf-powered coils for implant instruments," *Med. Biol. Eng. Comput.*, vol. 15, pp. 634–640, 1977.
- [4] J. C. Schuder, H. E. Stephenson, and J. F. Townsend, "High level electromagnetic energy transfer through a closed chestwall," *IRE Int. Conv. Rec.*, vol. 9, pp. 119–126, 1961.
- [5] E. Hochmair, "System optimization for improved accuracy in transcutaneous signal and power transmission," *IEEE Tran. Biomed. Eng.*, vol. BME-31, no. 2, pp. 177–186, Feb. 1984.
- [6] Y. Jang and M. M. Jovanovic, "A contactless electrical energy transmission system for portable-telephone battery chargers," *IEEE Tran. Ind. Electron.*, vol. 50, no. 3, pp. 520–527, Jun. 2003.
- [7] G. A. Covic and J. T. Boys, "Modern trends in inductive power transfer for transportation applications," *IEEE J. Emerg. Sel. Top. Power Electron.*, vol. 1, no. 1, pp. 28–41, May 2013.

- [8] U. K. Madawala and D. J. Thrimawithana, "A bidirectional inductive power interface for electric vehicles in V2G systems," *IEEE Tran. Ind. Electron.*, vol. 58, no. 10, pp. 4789–4796, Feb. 2011.
- [9] J. Huh, S. W. Lee, W. Y. Lee, G. H. Cho, and C. T. Rim, "Narrow-width inductive power transfer systems for online electrical vehicles," *IEEE Tran. Power Electron.*, vol. 26, no. 12, pp. 3666–3679, Dec. 2011.
- [10] S. Li and C. C. Mi, "Wireless power transfer for electric vehicle applications," *IEEE J. Emerg. Sel. Top. Power Electron.*, vol. 3, no. 1, pp. 4–17, Mar. 2015.
- [11] S. Y. R. Hui and W. C. Ho, "A new generation of universal contactless battery charging platform for portable consumer electronic equipment," *IEEE Tran. Power Electron.*, vol. 20, no. 3, pp. 620–627, May. 2005.
- [12] X. Liu and S. Y. R. Hui, "Simulation study and experimental verification of a contactless battery charging platform with localized charging features," *IEEE Tran. Power Electron.*, vol. 22, no. 6, pp. 2202–2210, Nov. 2007.
- [13] S. Y. R. Hui, "Planar inductive battery charging system," US Patent 7576514, Aug. 18, 2009.
- [14] Wireless Power Consortium (2018). [online]. Available: <http://www.wirelesspowerconsortium.com>.
- [15] S. Y. R. Hui, W. Zhong, and C. K. Lee, "A critical review of recent progress in mid-range wireless power transfer," *IEEE Tran. Power Electron.*, vol. 29, no. 9, pp. 4500–4511, Sept. 2014.
- [16] W. Zhong and S. Y. R. Hui, "Maximum Energy Efficiency Tracking for Wireless Power Transfer Systems," *IEEE Tran. Power Electron.*, vol. 30, no. 7, pp. 4025–4034, Jul. 2015.
- [17] Y. Yang, W. Zhong, S. Kiratipongvoot, S. C. Tan, and S. Y. R. Hui, "Dynamic Improvement of Series-Series Compensated Wireless Power Transfer Systems Using Discrete Sliding Mode Control," *IEEE Tran. Power Electron.*, vol. 33, no. 7, pp. 6351–6360, Jul. 2018.
- [18] Z. Wang, X. Lv, Y. Sun, X. Dai, and Y. Li, "A simple approach for load identification in current-fed inductive power transfer system," in *Proc. IEEE Int. Conf. Power Syst. Technol.*, 2012, pp. 1–5.
- [19] D. J. Thrimawithana and U. K. Madawala, "A primary side controller for inductive power transfer systems," in *Proc. IEEE IECON*, 2009, pp. 109–113.
- [20] Z. Wang, Y. Li, Y. Sun, C. Tang, and X. Lv, "Load detection model of voltage-fed inductive power transfer system," *IEEE Tran. Power Electron.*, vol. 28, no. 11, pp. 5233–5243, Nov. 2013.
- [21] J. Yin, D. Lin, T. Parisini, and S. Y. R. Hui, "Front-End Monitoring of the Mutual Inductance and Load Resistance in a Series-Series Compensated Wireless Power Transfer System," *IEEE Tran. Power Electron.*, vol. 31, no. 10, pp. 7339–7352, Oct. 2016.
- [22] E. X. Yang, F. C. Lee, and M. M. Jovanovic, "Small-signal modeling of series and parallel resonant converters," in *Proc. IEEE Appl. Power Electron. Conf.*, 1992, pp. 785–792.
- [23] N. A. Keeling, G. A. Covic, and J. T. Boys, "A unity-power-factor IPT pickup for high-power applications," *IEEE Tran. Ind. Electron.*, vol. 57, no. 2, pp. 744–751, Feb. 2010.
- [24] C. S. Wang, O. H. Stielau, and G. A. Covic, "Design considerations for a contactless electric vehicle battery charger," *IEEE Tran. Ind. Electron.*, vol. 52, no. 5, pp. 1308–1314, Oct. 2005.